

Diagnostic utility of ^{68}Ga - citrate and ^{18}F -FDG PET/CT in sarcoidosis patients

Cuneyt Tetikkurt¹, Halil Yanardag², Burcak Haluk Sayman³, Muammer Bilir², Seza Tetikkurt⁴, Seckin Bilgic³, Bahar Kubat¹, Seyda Bilgin²

¹Department of Pulmonary Medicine, Istanbul Cerrahpasa University, Istanbul; ²Department of Internal Medicine, Cerrahpasa Medical Faculty, Istanbul Cerrahpasa University, Istanbul; ³Department of Nuclear Medicine, Cerrahpasa Medical Faculty, Istanbul Cerrahpasa University, Istanbul; ⁴Department of Pathology, Demiroglu Bilim University Medical Faculty, Şişli/Istanbul, Turkey

Abstract

Sarcoidosis is a chronic granulomatous disease of unknown etiology. The disease most commonly involves the lungs and the mediastinal lymph nodes while extrapulmonary organs such as the skin, eye, liver or spleen may also be comprised. Many imaging modalities have been used for the clinical evaluation of sarcoidosis patients, but all have been found to have certain drawbacks for a reliable diag-

nostic assessment due to the equivocal diagnostic results. This study was designed to determine the clinical trenchancy of simultaneous ^{68}Ga -citrate PET/CT [Positron emission tomography with ^{68}Ga -citrate (^{68}Ga -citrate PET/CT)] and ^{18}F -FDG PET/CT [Positron emission tomography with 2-deoxy-2-[fluorine-18] fluoro-D-glucose (^{18}F -FDG PET/CT)] imaging in sarcoidosis patients. The main goal was to evaluate sarcoidosis patients with respect to diagnosis, disease activity and organ involvement. A total of eight sarcoidosis patients with a comorbid disease suspicion were included in the study. Conventional clinical parameters used for the diagnosis and the activity of sarcoidosis including clinical, laboratory and computed tomography (CT) manifestations were compared with the ^{68}Ga -citrate PET/CT findings. Concurrent ^{18}F -FDG PET/CT was performed to verify the granulomatous inflammation of sarcoidosis and to determine coexisting malignant or other inflammatory diseases. Our study results revealed that ^{68}Ga -citrate PET/CT imaging appears to be highly useful for the diagnosis, activity assessment and extrapulmonary organ involvement in sarcoidosis. Another crucial finding was the detection of extrapulmonary organ disease that are exceptionally involved, almost inaccessible by biopsy and that could not be otherwise displayed by other conventional imaging modalities. The third hallmark was the identification of a clinically asymptomatic and occult malignancy accompanying sarcoidosis that would not be detected in any way if synchronous ^{18}F -FDG PET/CT had not been performed. Simultaneous application of ^{68}Ga -citrate and ^{18}F -FDG PET/CT may provide extremely useful data for the clinical evaluation of sarcoidosis patients in terms of the primary disease diagnosis, activity state, extrapulmonary organ involvement unachievable for biopsy and revealing occult malignant disorders that may coexist with sarcoidosis.

Correspondence: Professor Cuneyt Tetikkurt, Department of Pulmonary Medicine, Istanbul Cerrahpasa University, Tanzimat Sok. Serkan Apt. No:8/16, 34728 Caddebostan, Istanbul, Turkey. Tel. +90.216.3601977. E-mail: tetikkurt@gmail.com

Key words: Sarcoidosis; ^{18}F -FDG PET/CT; ^{68}Ga -citrate PET/CT; malignancy.

Contributions: CT, pulmonary consultant for the cases and wrote the case series; HY, internal medicine consultant; HS, nuclear medicine consultant and prepared the nuclear medicine data; MB, wrote the clinical course of the patients; ST, wrote the pathologic aspects and mechanisms of sarcoidosis; SB, prepared the patient figure, composed the laboratory findings and the references; BK, wrote the clinical findings of the patients.

Conflicts of interest: The authors declare that they have no competing interests, and all authors confirm accuracy.

Ethics approval and consent to participate: No ethical committee approval was required for this case report by the Department, because this article does not contain any studies with human participants or animals. Informed consent was obtained from the patients included in this study.

Availability of data and materials: All data generated or analyzed during this study are included in this published article.

Received for publication: 15 July 2020.
Accepted for publication: 10 November 2020.

©Copyright: the Author(s), 2020
Licensee PAGEPress, Italy
Monaldi Archives for Chest Disease 2020; 90:1509
doi: 10.4081/monaldi.2020.1509

This article is distributed under the terms of the Creative Commons Attribution Noncommercial License (by-nc 4.0) which permits any noncommercial use, distribution, and reproduction in any medium, provided the original author(s) and source are credited.

Introduction

Sarcoidosis is a chronic granulomatous disorder of unknown origin characterized by the presence of non-caseified granulomas in various organs with an approximately 95% lung involvement while lymph nodes, eyes and skin are other commonly involved sites [1-4]. Frequently used imaging modalities to identify sarcoidosis and organ involvement may reveal contentious or disputable results in terms of these two aforementioned criteria. Unfortunately, the recently introduced Positron emission tomography with 2-deoxy-2-[fluorine-18] fluoro-D-glucose (^{18}F -FDG PET/CT) have not yielded the optimal results for diagnosis and detection of disease activity providing a low diagnostic accuracy. Novel radiopharmaceuticals aimed at other disease targets may be conducive, particularly in car-

diac sarcoidosis such as the ^{68}Ga -citrate PET/CT. ^{68}Ga -labeled somatostatin-based receptor hybrid imaging appears to be a significant alternative to ^{18}F -FDG PET/CT, ^{67}Ga -citrate scintigraphy, computed tomography (CT) to identify disease activity and organ involvement in sarcoidosis patients [5-7]. ^{68}Ga -labeled somatostatin-based receptor hybrid imaging now is reported as a powerful diagnostic procedure for sarcoidosis [1-3]. This considerably new imaging modality has evidently become a useful screening tool to assess the disease activity and treatment response revealing a high sensitivity and a specificity of 92.5% and 83.3%, respectively for sarcoidosis patients [7-10]. Alternatively, ^{68}Ga -citrate having similar chemical properties with ^{67}Ga -citrate and also providing lower radiation doses, may be used to achieve higher image resolution of PET/CT scanners compared to conventional gamma cameras for the same purpose. Initially, the application of ^{68}Ga -citrate was not promising since the traditional ^{67}Ga -citrate images were obtained far beyond the physical half-life of ^{68}Ga -citrate and consequently the application of ^{68}Ga -citrate was discarded for some time. As a homolog of ferric cation ^{68}Ga -citrate is bound to plasma proteins and the blood content is high up to two hours. Therefore, it would be a rational approach to compare the ^{68}Ga -citrate uptake in the lymph nodes to blood in order to regard this imaging appearance pathological for sarcoidosis. In the current study, we present eight patients in whom ^{68}Ga -citrate PET/CT was used simultaneously with ^{18}F -FDG PET/CT for the identification of sarcoidosis, disease activity, extrapulmonary organ involvement and for the diagnosis of other accompanying malignant disorders.

^{68}Ga -citrate PET/CT appears to be a crucial guide as an imaging modality for the clinicians by revealing extremely useful clinical data in all aspects of sarcoidosis including diagnosis, current disease activity and for the identification of extrapulmonary organ sarcoidosis that is difficult and even inaccessible for biopsy due to its location. On the other hand, the concurrent use of ^{18}F -FDG PET/CT has provided beneficial results for the identification of comorbid diseases, especially coexisting asymptomatic and occult malignancy in these patients.

Case #1

A 56-year-old female was admitted for double vision complaint in the right eye. Her personal and family history were unremarkable except for hypertension. Physical examination revealed normal system and vital findings other than the double vision in the right eye. Complete blood count was within normal limits. CRP

was 16.49 mg/L and antithyroglobulin was 675.8 IU/ml. Serum ACE was high while serum and urinary calcium were normal (Table 1). Chest X-ray showed bilateral enlarged hilar lymph nodes and parenchymal infiltrations in both upper lobes. Tuberculin test was negative. Pulmonary function tests and DLCO/VA demonstrated normal values. Thorax CT revealed ground-glass infiltrations with a mosaic pattern in both lungs and bilateral hilar lymphadenopathy. Cranial MR showed a 12x8x17 mm lesion while ^{68}Ga -citrate PET/CT revealed increased uptake (SUV_{max} : 3.85) at the right posterior cavernous sinus (Figure 1) compatible with sarcoidosis. ^{18}F -FDG PET/CT demonstrated increased ^{18}F -FDG avidity (SUV_{max} : 3.3) in the right posterior cavernous sinus lesion. Transbronchial biopsy revealed non-caseified granulomatous inflammation while BAL demonstrated lymphocytosis with a high CD_4/CD_8 ratio (Table 2). The final diagnosis was stage II sarcoidosis with neurologic involvement. Following 32 mg/day methylprednisolone treatment the patient had an uneventful recovery with complete resolution of her symptoms.

Case #2

A 42-year-old male presented with a two months history of lassitude, headache and arthralgia. Personal history included sarcoidosis of four years and thyroid carcinoma resection six years ago. Family history revealed sarcoidosis in the father and the sibling. His vital signs and physical examination revealed a blood pressure of 130/75 mm Hg, a heart rate of 92 beats/min and a respiratory rate of 12 breaths/min. He was not on any regular medications. Blood count, serum biochemistry, serum ACE, calcium and urinary calcium complete blood count were within normal limits (Table 1). Tuberculin test was negative. Pulmonary function tests revealed a mild decrease in FVC and DLCO/VA. Chest X-ray showed bilateral infiltrations in the upper and middle lung zones. Thorax CT revealed alveolar parenchymal infiltrations in both upper lobes, middle lobe and lingula. BAL analysis demonstrated lymphocytosis with an increased CD_4/CD_8 ratio (Table 2) compatible with active sarcoidosis. BAL culture was negative for bacteria, fungus and mycobacteria. Ocular examination demonstrated anterior uveitis. Cranial MR T1 image demonstrated a 24x14x20 mm lesion at the left orbital base with moderate enhancement. ^{18}F -FDG and ^{68}Ga -citrate PET/CT (Figure 2) revealed a 24 mm left orbital nodule with high avidity compatible with granulomatous inflammation (Table 2). Final diagnosis was stage III sarcoidosis and associated left orbital granuloma.

Table 1. Clinical and basic laboratory manifestations of the patients.

Patient	Gender and age	Initial symptom	Organ(s) involved with sarcoidosis	Serum ACE (U/L)	Serum Ca (mg/dl)	Urinary Ca (mg/day)
# 1	F, 56	Double vision in the right eye	Lung and right sinus cavernosus	94	9.2	240
# 2	M, 42	Lassitude, headache and arthralgia	Lung, eye and left orbit	24	9.6	286
# 3	F, 48	Dyspnea on exertion, lassitude and myalgia	Bilateral hilar and mediastinal lymph nodes	18	9.8	278
# 4	F, 52	Dry cough and weight loss	Lung, eye and mediastinal lymph nodes	86	9.4	256
# 5	F, 46	Dyspnea, arthralgia and lassitude	Lung, mediastinal lymph nodes and eye	32	9.5	236
# 6	M, 64	Dry cough, lassitude and maculopapular rash	None	50	10.2	294
# 7	F, 39	Fatigue, dry cough and arthralgia	Lung, right supraclavicular and bilateral hilar lymph nodes	42	9.1	274
# 8	M, 58	Lassitude and confusion	Lung, right orbit and mediastinal lymph nodes	82	17.5	340

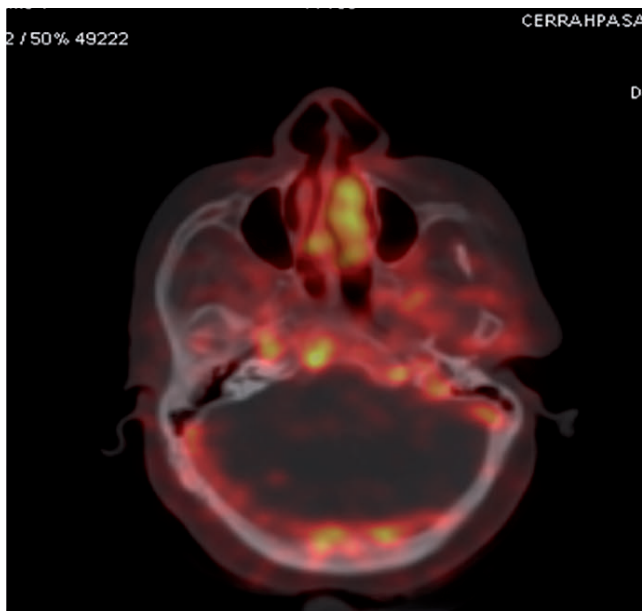


Figure 1. ⁶⁸Ga-citrate PET/CT revealing significantly increased avidity within a granulomatous lesion at the right posterior cavernous sinus.

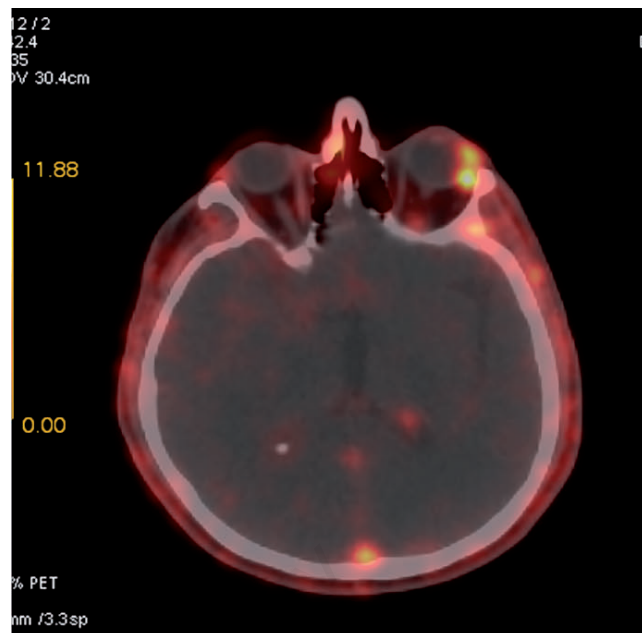


Figure 2. ⁶⁸Ga-citrate PET/CT showing a focal granuloma with distinctive uptake at the left anterior orbita.

Table 2. Pulmonary function, imaging, bronchoscopy, ⁶⁸Ga-citrate and ¹⁸F-FDG PET/CT findings of the patients.

Patients	PFT and DLCO/VA	Chest X-ray and stage	Thorax CT	TBB and BAL	¹⁸ F-FDG PET/CT	⁶⁸ Ga-citrate PET/CT
# 1	FVC: 82% DLCO/VA: 80%	Bilateral infiltrations in the upper lobes and BHL	BHL, bilateral GG and MP infiltrations the upper and middle lobes	NCGI Lymphocytosis and 4.6	↑ ¹⁸ F-FDG uptake in the right sinus cavernosus	↑ ⁶⁸ Ga-citrate avidity in the right sinus cavernosus
# 2	FVC: 78% DLCO/VA: 67%	Bilateral infiltrations in the upper, middle lobe and lingula Stage III	Bilateral alveolar infiltrations in the upper, middle lobe and lingula	Not done Lymphocytosis and 4.0	↑ ¹⁸ F-FDG avidity in the left anterior orbit	↑ ⁶⁸ Ga-citrate uptake in the left anterior orbit
# 3	FVC: 80% DLCO/VA: 84%	BHL Stage I	BHL and mediastinal lymphadenopathy	NCGI Lymphocytosis and 2.8	↑ ¹⁸ F-FDG uptake in the hilar and mediastinal lymph nodes	↑ ⁶⁸ Ga-citrate avidity in the hilar and mediastinal lymph nodes
# 4	FVC: 72% DLCO/VA: 76%	BHL and lung nodules Stage II	Pulmonary parenchymal nodules, BHL and enlarged mediastinal lymph nodes	Not done Lymphocytosis and 3.8	↑ ¹⁸ F-FDG avidity in the hilar and mediastinal lymph nodes	↑ ⁶⁸ Ga-citrate uptake in the hilar and mediastinal lymph nodes
# 5	FVC: 68% DLCO/VA: 72%	Infiltrations in the upper lobes of both lungs Stage III	Bilateral alveolar upper and middle lobe infiltrations	NCGI 2.4	Physiologic ¹⁸ F-FDG avidity in the lung, mediastinum and pathologic uptake in the right orbital wall	Physiologic ⁶⁸ Ga-citrate uptake in the lung and mediastinum
# 6	FEV1: 64% DLCO/VA: 82%	Lung Stage 0	Nodule in the left upper division lobe and left lower atelectasis segment	GI 2.0	↑ ¹⁸ F-FDG uptake in the left upper lobe and left lower abdominal quadrant	Physiologic ⁶⁸ Ga-citrate avidity in the lung and mediastinum
# 7	FVC: 70% DLCO/VA: 74%	Bilateral nodules and BHL Stage II	Bilateral pulmonary parenchymal nodules and BHL	NCGI Lymphocytosis and 4.8	↑ ¹⁸ F-FDG avidity in the lung parenchyma and hilar lymph nodes	↑ ⁶⁸ Ga-citrate uptake in the lung parenchyma and hilar lymph nodes
# 8	FEV1: 76% DLCO/VA: 59%	Bilateral infiltrations in the upper lobes Stage II	Alveolar infiltrations in the upper, middle lobe and lingula	NCGI Lymphocytosis and 2.8	↑ ¹⁸ F-FDG uptake in the lungs, mediastinum, left leg muscles, pubis, ischium bones and right orbit	↑ ⁶⁸ Ga-citrate avidity in the lungs, mediastinum and right orbit

ACE, angiotensin converting enzyme; BHL, bilateral hilar lymphadenopathy; GG, ground glass; MP, mosaic pattern; NCGI, non-caseified granulomatous inflammation; GI, granulomatous inflammation; rsc, right sinus cavernosus.

Case #3

A 48-year-old female was referred for dyspnea on exertion, lassitude and myalgia of three months. The patient noted that previous treatment with inhaled steroids was not useful. She had a medical history of cholecystectomy four years ago with no significant disease in the family history. Physical examination demonstrated a blood pressure of 120/70 mm Hg, a heart rate of 82 beats/min and a respiratory rate of 14 breaths/min. Complete blood count, serum biochemistry, serum ACE, calcium and urinary calcium were within normal limits (Table 1). Tuberculin test was negative. Chest X-ray and thorax CT revealed bilateral hilar and mediastinal enlarged lymph nodes. Pulmonary function tests demonstrated normal FVC and DLCO/VA values. Pathology of the transbronchial biopsy specimen revealed non-caseified granulomatous inflammation. BAL cell count showed lymphocytosis and a normal CD4/CD8 (Table 2) ratio while lavage culture was negative for bacteria, fungus or mycobacteria. Ophthalmologic examination did not reveal any pathologic findings. ¹⁸F-FDG and ⁶⁸Ga-citrate PET/CT showed high tracer avidity in the hilar and mediastinal lymph nodes (Table 2). Final diagnosis was stage I sarcoidosis.

Case #4

A 52-year female was admitted for dry cough and 10 kg weight loss in the last six months. She had a past medical history of hypertension, gastric ulcer, sarcoidosis and associated uveitis of twelve years. Physical examination was unremarkable except for a blood pressure of 180/95 mm Hg. Complete blood count, serum biochemistry and urine analysis were normal. Tuberculin test was negative. Serum and urinary calcium levels were within normal limits while serum ACE was high (Table 1). Bilateral hilar lymphadenopathy and parenchymal nodules were present on chest X-ray. Pulmonary function tests demonstrated a mild restrictive pattern with a mild decrease in DLCO/VA value. Thorax CT revealed parenchymal and subpleural nodules in both lungs at the upper, middle, lingular lobes with bilateral enlarged hilar and mediastinal lymph nodes varying between 15 and 20 mm in short axis diameter compatible with stage II sarcoidosis. BAL revealed lymphocytosis and a high CD4/CD8 ratio (Table 2) while culture was negative for bacteria, fungus and mycobacteria. Ocular examination showed intermediate uveitis. ¹⁸F-FDG and ⁶⁸Ga-citrate PET/CT showed multiple hypermetabolic foci in both hilar, carinal and subcarinal lymph nodes (Table 2). Final diagnosis was stage II sarcoidosis.

Case #5

A 46-year-old female presented with dyspnea, arthralgia and lassitude for six weeks. Her medical history included sarcoidosis of eight years and a surgical operation for right kidney nephrolithiasis five years ago. Family history did not reveal any significant disease. She had been commenced on a six-month methylprednisolone treatment for sarcoidosis previously and was not on any regular medications currently. Physical examination manifested a blood pressure of 110/70 mm Hg, heart rate of 82 beats/min and a respiratory rate of 14 breaths/min. Complete blood count, serum biochemistry, urine analysis, acute phase reactants other than ESR (72 mm/h) and rheumatologic panel were within normal limits. Tuberculin test was

negative. Serum ACE, serum and urinary calcium revealed normal levels (Table 1). Chest X-ray showed infiltrations in the upper lobes of both lungs. Pulmonary function tests demonstrated a mild restrictive defect with a mild decrease in DLCO/VA. Chest CT showed infiltrative lesions in the upper and middle lobes. Histopathology of the transbronchial lung biopsy revealed non-caseified granulomatous inflammation compatible with sarcoidosis. BAL cell count, differential cytology and CD4/CD8 ratio revealed normal findings (Table 2). BAL culture was negative for bacteria, fungus and mycobacteria. Ophthalmologic examination demonstrated anterior uveitis. ¹⁸F-FDG and ⁶⁸Ga-citrate PET/CT showed physiologic uptake in the lung and mediastinum while right orbital wall revealed increased FDG avidity (Table 2). Final diagnosis was stage III sarcoidosis.

Case #6

A 64-year-old male was referred for the evaluation of dry cough, lassitude and maculopapular rash of two weeks on the anterior chest wall. Past medical history included sarcoidosis and psoriasis. Physical examination revealed a blood pressure of 120/80 mm Hg, a heart rate of 86/min, a respiratory rate of 16/min and a maculopapular rash on the anterior chest wall. Blood count, serum biochemistry and rheumatologic screening were unremarkable. Serum and urinary calcium levels were within physiologic levels. Serum ACE level was normal (Table 1). Chest x-ray showed normal parenchymal and mediastinal findings. Spirometry demonstrated moderate airflow obstruction and a normal DLCO/VA. Tuberculin test was negative. Thorax CT revealed a nodule in the left upper division bronchus orifice and two nodules in the lateral segments of both lower lobes. ¹⁸F-FDG PET/CT demonstrated moderate ¹⁸F-FDG uptake in the left upper division and in the left lower lobe laterobasal segment nodules with SUVmax of 2.9, diffuse ¹⁸F-FDG avidity in the major vessels with an incidental left lower abdominal quadrant lesion of 18 mm with a SUVmax of 18.2 (Figure 3a,3b) which was later proved to be colon adenocarcinoma. ⁶⁸Ga-citrate PET/CT did not show active granulomatous inflammation relevant to sarcoidosis in the lung, mediastinum or in any other organ (Table 2). Dermatology consultation concluded that the maculopapular rash was associated with psoriasis exacerbation. The high ¹⁸F-FDG uptake in the major vessels was evaluated as vasculitic changes due to psoriasis. Bronchoscopy demonstrated funnel-shaped narrowing of the left upper division and two gray colored submucosal nodules at the right middle lobe orifice. Pathology of the bronchoscopic biopsy samples revealed non-specific granulomatous inflammation due to anthracosis. BAL cell count and differential cytology profile was normal (Table 2), while culture did not grow any bacteria, fungus or mycobacteria. Histopathology of the EBUS biopsy samples from 4R and 11L lymph nodes revealed anthracosis. Pathologic examination of the colon biopsy specimen identified low-grade adenocarcinoma. Final diagnosis was psoriasis, sarcoidosis and colon carcinoma. The patient had an uneventful colectomy.

Case #7

A 39-year-old female was admitted for fatigue, dry cough and arthralgia of six weeks. She was a non-smoker. Personal and family history did not reveal any significant disease. Physical examination demonstrated a blood pressure of 110/70 mm Hg, a heart

rate of 82/min, a respiratory rate of 14/min at rest and a right supraclavicular lymph node. Complete blood count, liver and renal function tests were normal. Tuberculin test was negative. Serum ACE, serum and 24/h urinary Ca levels were within normal levels (Table 1). Chest X-ray and thorax CT showed bilateral pulmonary nodular opacities and bilateral enlarged hilar lymph nodes. Pulmonary function tests demonstrated a mild restrictive function and a mild DLCO/VA defect. Histopathologic examination of the right supraclavicular and the transbronchial biopsy samples revealed non-caseified granulomatous inflammation while BAL cytology showed lymphocytosis with a high CD₄/CD₈ ratio (Table 2) compatible with sarcoidosis. ¹⁸F-FDG and ⁶⁸Ga-citrate PET/CT revealed mildly increased avidity in the parenchymal lung lesions and the hilar lymph nodes (Table 2). Final diagnosis was stage II sarcoidosis.

Case #8

A 58-year-old male was admitted for lassitude and confusion of ten days. He was a never smoker with a 32 years of sarcoidosis disease. Family history did not reveal any disorder of significance. Physical examination and vital findings were normal other than the drowsy state of the patient. A five-centimeter solid lesion was palpated at the back side of the left upper leg. Serum ACE, serum and daily urine calcium were high above normal (Table 1). Chest X-ray showed infiltrative changes in the upper lobes. Tuberculin test was negative. Spirometry showed mild obstructive disease with a moderately decreased DLCO/VA value. Chest CT demonstrated alveolar opacities in both upper lobes, middle lobe and lingula. BAL fluid examination showed lymphocytosis and a normal CD₄/CD₈ ratio. Volume expansion with saline 200 ml/h, zoledronic acid 4 mg and 32 mg/day methylprednisolone were commenced for sarcoidosis and associated hypercalcemia. ¹⁸F-FDG PET/CT revealed diffuse tracer uptake in the lungs, mediastinum, left gemellus, left adductor, left external abdominalis oblique muscles, both pubis and ischium bones with a focal uptake (SUV: 5.29) in the medial

wall of the right orbit (Table 2). ⁶⁸Ga-citrate PET/CT showed increased tracer avidity in the lungs, mediastinum and right orbit (Figure 4a,b,c). Brain diffusion MR revealed age related ischemic vascular changes in both cerebral hemispheres. Histopathology of the transbronchial biopsy specimen revealed non-caseified granulomatous inflammation while muscle biopsy pathology disclosed B-cell lymphoma. The final diagnosis was stage II sarcoidosis and B-cell lymphoma.

Discussion

Sarcoidosis is a disease of unknown origin characterized by the presence of non-caseified granulomas most commonly in the lungs while any other extrapulmonary organ including the lymph nodes, eyes or skin may also be involved. Given the clinical profile of sarcoidosis, it is obvious that none of the body organs is immune against sarcoidosis [8-10]. Currently, various imaging modalities are used for the diagnosis of sarcoidosis, disease activity and identification of extrapulmonary organ involvement. None of these procedures have achieved adequate sensitivity and specificity for the diagnosis or assessment of sarcoidosis. Likewise, ⁶⁷Ga-citrate scintigraphy has not yielded the desired diagnostic yield in terms of clinical practice [11-14]. The ¹⁸F-FDG PET/CT has emerged as a useful adjunct for identifying pulmonary or extrapulmonary organ sarcoidosis, disease activity and revealing targets for tissue diagnosis but it also has been reported to exhibit variable sensitivity and specificity for clinical evaluation [6,11-13]. On the other hand, detection of extremely high somastatin receptor activity in sarcoid granulomas has led to the idea that somastatin scintigraphy may provide useful data for the diagnosis of sarcoidosis patients nowadays.

In some recent studies, it has been shown that the ⁶⁸Ga somatostatin receptor PET/CT which is primarily used for oncological diagnosis may also be an influential imaging procedure for the evaluation of sarcoidosis patients due to the high expression of somatostatin receptor subtype 2 in sarcoid granulomas [4-6]. Instead of using somatostatin receptor imaging, ⁶⁸Ga-citrate was

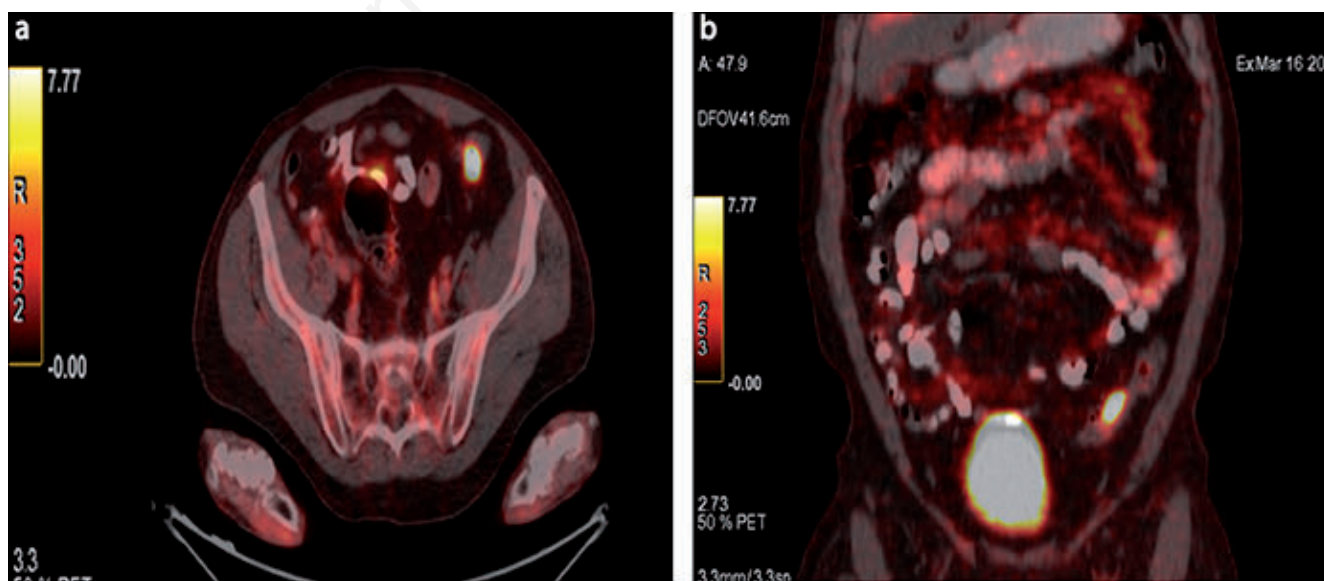


Figure 3. Axial (a) and coronal (b) ¹⁸F-FDG PET/CT fusion image revealing a high FDG uptake at the left lower quadrant lesion.



Figure 4. ^{68}Ga -citrate PET/CT images showing increased tracer uptake in the left leg muscles, right orbit and right lung parenchyma.

utilized in these cases to determine diagnosis, disease activity and extrapulmonary organ involvement as well as the diagnostic yield of simultaneous ^{18}F -FDG use in sarcoidosis patients. A final diagnosis of left orbital and a right posterior cavernous sinus sarcoidosis granuloma was reached by simultaneous application of these imaging modalities that was otherwise almost impossible to be identified by the application of conventional imaging techniques, clinical methods or invasive procedures like biopsy in one of our patients. The results of our study indicate that the concurrent application of these two imaging modalities will not only provide significant data for disease diagnosis and activity but also will identify extrapulmonary organ involvement sites thereby leading the clinician in the correct the diagnostic pathway for sarcoidosis. In another sarcoidosis patient of this case series, a clinically occult and asymptomatic colon carcinoma was detected by the simultaneous application of ^{18}F -FDG and ^{68}Ga -citrate PET/CT. The other hallmark of our study was the diagnosis of a silent malignancy accompanying sarcoidosis with the use of two different imaging modalities.

It is well-known that clinicians experience great difficulties for the identification of active disease and extrapulmonary organ involvement in sarcoidosis patients. Unfortunately, the current laboratory and imaging modalities have not been able to reach an adequate sensitivity and specificity in terms of diagnosis, activity assessment and extrapulmonary organ involvement. Laboratory innovations have focused on the lung, which is the most commonly affected organ in sarcoidosis. Although many different procedures are used to determine the activity of pulmonary sarcoidosis, they occasionally remain insufficient for an indubitable diagnosis. When active granulomatous inflammation occurs in extrapulmonary organs, the current conventional methods are even more inconclusive than detecting active lung disease. This lack of diagnostic sensitivity and specificity especially exists for vital organs like the heart or the central nervous system and for the end organs such as the parotid or lacrimal gland where the presence of granulomatous disease may easily be missed. This case series has clearly demonstrated the extremely beneficial effects of these imaging modalities in the diagnosis of sarcoidosis, the detection of active granulomatous inflammation in the extrapulmonary organs and as well as the identification of clinically occult coexisting malignant diseases. We believe that the further development of such interventions may also eliminate the necessity of organ biopsy for diagnosis and detection of organ involvement.

In two patients, active granulomatous inflammation was detected by the presence of a high serum calcium in one and a high serum ACE value in the other. The high serum calcium and the high ACE values in these patients are caused by the metabolic activity of the granulomas. ^{18}F -FDG or ^{68}Ga -citrate PET/CT did not reveal any increased tracer uptake or avidity in these subjects. The metabolic activity of sarcoidosis could not be identified by the aforementioned nuclear imaging modalities. The main reason for the ^{18}F -FDG and ^{68}Ga -citrate imaging failure to detect the granulomatous inflammatory activity is most likely associated with the inadequate tracer avidity due to the small size of the granulomatous lesions in sarcoidosis patients. The granulomatous lesions were not detected because they were far beyond the limit of either ^{18}F -FDG or ^{68}Ga -citrate PET/CT resolution. Consequently, the ^{18}F -FDG and ^{68}Ga -citrate PET/CT yielded equivocal findings in terms of disease activity or organ involvement in these cases. While the size limit accepted for the detection of malignant lesions by ^{18}F -FDG or ^{68}Ga -citrate PET/CT varies between 8 to 10 mm, a predetermined criterion for the designation of inflammatory or granulomatous lesions by dimension is not available currently. On

the other hand, conventional serum activity markers of sarcoidosis revealed full compatibility with the ^{68}Ga -citrate uptake and avidity in three other patients. The ^{18}F -FDG and ^{68}Ga -citrate PET/CT tracer uptake primarily depends upon the extent of granulomatous inflammation whereas small inflammatory areas less than ten millimeters may not demonstrate visible tracer acquisition while larger lesions reveal increased tracer avidity. This phenomenon seems to be relevant with the fact that patients with stage 0 sarcoidosis without any visible lesions on the chest X-ray may have a high serum ACE, hypercalcemia, BAL lymphocytosis, an increased CD_4/CD_8 ratio, and the presence of non-caseified granulomas in the transbronchial specimens as the granulomatous lung inflammation is beyond the radiologic resolution due to their small size [15,16]. In conclusion, the lesion size appears to be the determinant factor that ascertains the diagnostic efficiency of these two imaging modalities for sarcoidosis patients. Since the extent of the granulomatous lesion or inflammation is the most important coefficient for demonstrating organ involvement or disease activity for nuclear imaging modalities, this condition appears to be the most crucial limitation of these screening procedures. Further studies are needed to establish the decisive minimal dimension for benign inflammatory granulomatous lesions of sarcoidosis.

There are some limitations of our case series. The first drawback is the small sample size consisting of only eight patients as a preliminary study. The small sample size is associated with the fact that ^{68}Ga -citrate PET/CT is an imaging modality initially performed primarily for oncologic diagnosis while its use in sarcoidosis patients is relatively recent. All patients included in our case series were of Caucasian origin. It is well-known that sarcoidosis patients may exhibit variable profiles according to their racial characteristics in terms of disease onset, laboratory findings, imaging manifestations, clinical course, prognosis and treatment response due to the distinct genetic features. Studies with larger sample sizes comprising distinct genetic profiles or characteristics are required to yield more explicit data. Although the application of two different imaging modalities simultaneously may lead to an economic burden, it should not be forgotten that in the long term, the investigation of a patient for possible malignant and inflammatory diseases may cause a much greater financial burden. Furthermore, the assessment of such patients would also be more time consuming almost with an equal expense delaying the final diagnosis and treatment as well.

Somatostatin analogs used in PET/CT show different affinity for different SSTR receptor subtypes. ^{68}Ga -DOTANOC reveals a high affinity for both SSTR2 and SSTR5 whereas ^{68}Ga -DOTATOC has mainly a high affinity to SSTR2 [4,6,17,18]. While the SSTR2 is highly expressed in sarcoid granulomas [4,5] it is currently unknown whether other somatostatin receptor types also exist in the granulomatous lesions of sarcoidosis. Incompatibility between the existing somatostatin receptors of sarcoidosis granulomas and the PET imaging tracers may be considered as the most crucial drawback for the PET/CT imaging modalities in terms of diagnostic accuracy. With the identification of yet unknown somatostatin receptors in sarcoidosis granulomas and the introduction of new radioactive tracers for them, will further advance the diagnostic yield of these procedures for the individual patient.

Immunosuppressive and anti-inflammatory features of gallium compounds have been demonstrated in animal models of human diseases. Radioactive gallium is used as a diagnostic and a therapeutic agent in cancer, disorders of bone and calcium metabolism. Following high continuous infusion gallium doses, adverse effects such as diarrhea, renal toxicity and visual or auditory toxicities

may occur in 12.5% and 1% of the patients, respectively [19,20]. There is no data in the literature revealing that a significant short-term or long-term side effects of a single ^{18}F -FDG or ^{68}Ga -citrate application performed as an imaging modality. Likewise, there are not any serious adverse impacts for double or simultaneous administration of ^{18}F -FDG and ^{68}Ga -citrate tracers used as an imaging utility [19-24]. Although potential hazards may come out due to the cumulative radioactive doses of simultaneous ^{18}F -FDG and ^{68}Ga -citrate application, data relevant to such adverse effects has not been stated by now. Concisely, double application of these two imaging modalities does not lead to any short-term potential toxicity while the long-term sequela of this integrated application is currently unknown. Since data relevant to the long-term toxic or adverse effects for the cumulative dose of simultaneous ^{18}F -FDG and ^{68}Ga -citrate PET/CT imaging are not available, further studies are required to determine the potential hazards of this application more definitely.

The existence of active granulomatous inflammation in sarcoidosis patients may be easily missed with the current clinical laboratory and imaging tools. It is well-known that the more tests are performed for diagnosis, the higher the diagnostic sensitivity and the specificity will be as it is the case in the separation of exudative and transudative pleural effusions by Light's criteria [25]. Inclusion of albumin gradient, cholesterol level and bilirubin ratio has further increased the diagnostic sensitivity and specificity for the identification of exudative pleural fluids [26-28]. On the other hand, when rheumatological markers, differential cell count and cytology are used, the final diagnosis is achieved much more accurately for pleural effusions. The cardinal objective of our case series was to increase the sensitivity and specificity of imaging modalities concerning the diagnosis, disease activity and determination of extrapulmonary organ involvement by using two different imaging modalities. Detection of extrapulmonary disease has provided clinicians with a valuable opportunity of easy-to-access biopsy sites to proceed on the right diagnostic pathway for the final diagnosis of sarcoidosis.

The variable inflammatory response and the inconsistent organ involvement in sarcoidosis patients necessitate the implementation of distinctive imaging procedures for more definitive and conclusive results in clinical practice that facilitate and thereby speed up the final diagnosis. Since active granulomatous inflammation of sarcoidosis may easily be missed by the currently available laboratory tests and the imaging modalities, performing two distinctive screening procedures simultaneously will increase the diagnostic sensitivity and specificity considerably by identifying the granulomatous inflammation in these patients. Concurrent administration of two different imaging modalities will provide the clinicians with much more precise data for the granulomatous inflammation of the primary disease as well as the vitally requisite disorders such as the coexisting malignancy. Diagnosis of an asymptomatic and clinically occult malignant disease with ^{18}F -FDG PET/CT is perhaps one of the most indispensable points of this study that justifies the complementary use of these two procedures in patients with suspected malignancy.

Synchronous use of two imaging modalities has identified active inflammation foci as well as the presence of granuloma in two different localizations that are rarely involved in sarcoidosis. In addition to the identification of these exceptionally unusual granulomatous foci that are almost impossible to biopsy, the elimination of the biopsy exigence for diagnosis is the other hallmark of our study. Utility of two different PET imaging modalities simultaneously has facilitated the final diagnosis by precluding further delay. Such an approach is particularly valuable in sar-

coidosis patients for determining disease activity in terms of ongoing granulomatous inflammation and accelerating the diagnosis by detecting the involved organs to confirm the requisite biopsy sites for the final diagnosis. ^{68}Ga -citrate and ^{18}F -FDG PET/CT have revealed compatible results with the currently applied conventional laboratory methods that define the activity of sarcoidosis. Detection of an occult malignancy and the identification of sarcoidosis foci that are almost inaccessible by biopsy with these imaging modalities are the most important triangulation points of this case series. Although many biomarkers have been used to identify the activity status of sarcoidosis patients none of these has revealed satisfactory sensitive and specific consequences in clinical practice. Our study results suggest that these two imaging modalities can be used as activity markers of granulomatous inflammation in sarcoidosis as well as the other diagnostic benefits mentioned above.

Conclusions

^{68}Ga -citrate appears to be a useful imaging tool for sarcoidosis patients because of its ability to identify disease activity, to detect organ involvement and to localize biopsy sites for a final diagnosis. The simultaneous use of these two screening procedures may serve as an extremely useful diagnostic modality for sarcoidosis patients and such an application is therefore beneficial to exclude a currently active inflammatory state of sarcoidosis to which the present symptoms of a patient are primarily attributed to preexisting disease leading the clinician in the correct diagnostic pathway. Determination of easily accessible biopsy areas and avoiding biopsy areas that are almost impossible to reach is another hallmark of this study.

On the other hand, diagnosis of an occult malign disease by simultaneous use of ^{18}F -FDG PET/CT is the fundamental aspect of our findings. The last point is that the more tests performed in a patient, the higher the diagnostic sensitivity and specificity will be, which is especially true for the imaging modalities that may replace many laboratory methods for sarcoidosis in the near future. Clinicians should bear in mind that the threshold that will determine the diagnostic yield of these imaging modalities is the dimension of the granulomatous lesions of the involved pulmonary and extrapulmonary organs. The concurrent application of ^{18}F -FDG and ^{68}Ga -citrate PET/CT in patients with suspected or previously known sarcoidosis may reveal excessively useful data in terms of sarcoidosis diagnosis, determination of disease activity, detection of involved organs unachievable for biopsy and for the identification of clinically occult malignancy in these patients.

References

- Slart RHJA, Koopmans KP, van Geel PP, et al. Somatostatin receptor based hybrid imaging in sarcoidosis. *Eur J Hybrid Imaging* 2017;1:1-5.
- Sharma S, Singh AD, Sharma SK, et al. Gallium-68 DOTA-NOC PET/CT as an alternate predictor of disease activity in sarcoidosis. *Nucl Med Commun* 2018;39:768-78.
- Youssef G, Leung E, Mylonas I, et al. The use of ^{18}F -FDG PET in the diagnosis of cardiac sarcoidosis: a systematic review and metaanalysis including the Ontario experience. *J Nucl Med* 2012;53:241-8.
- Kamphuis LS, Kwekkeboom DJ, Missotten TO, et al. Somatostatin receptor scintigraphy patterns in patients with sarcoidosis. *Clin Nucl Med* 2015;40:925-9.
- Lapa C, Reiter T, Kircher M, et al. Somatostatin receptor based PET/CT in patients with the suspicion of cardiac sarcoidosis: an initial comparison to cardiac MRI. *Oncotarget* 2016;7:77807-14.
- Nobashi T, Nakamoto Y, Kubo T, et al. The utility of PET/CT with $(^{68}\text{Ga})\text{Ga}$ -DOTATOC in sarcoidosis: comparison with $(^{67}\text{Ga})\text{Ga}$ -scintigraphy. *Ann Nucl Med* 2016;30:544-52.
- Baughman RP, Teirstein AS, Judson MA, et al. Clinical characteristics of patients in a case control study of sarcoidosis. *Am J Respir Crit Care Med* 2001;164:1885-9.
- [No authors listed]. Statement on sarcoidosis. Joint Statement of the American Thoracic Society (ATS), the European Respiratory Society (ERS) and the World Association of Sarcoidosis and Other Granulomatous Disorders (WASOG) adopted by the ATS Board of Directors and by the ERS Executive Committee, February 1999. *Am J Respir Crit Care Med* 1999;160:736-55.
- Costabel U, Hunninghake GW. ATS/ERS/WASOG statement on sarcoidosis. Sarcoidosis Statement Committee. American Thoracic Society. European Respiratory Society. World Association for Sarcoidosis and Other Granulomatous Disorders. *Eur Respir J* 1999;14:735-7.
- Hunninghake GW, Costabel U, Ando M, et al. ATS/ERS/WASOG statement on sarcoidosis. American Thoracic Society/European Respiratory Society/World Association of Sarcoidosis and other Granulomatous Disorders. *Sarcoidosis Vasc Diffuse Lung Dis* 1999;16:149-73.
- Keijsers RG, Grutters JC, Thomeer M et al. Imaging the inflammatory activity of sarcoidosis: sensitivity and inter observer agreement of $(^{67}\text{Ga})\text{Ga}$ imaging and $(^{18}\text{F})\text{F}$ -FDG PET. *Q J Nucl Med Mol Imaging* 2011;55:66-71.
- Prager E, Wehrschoetz M, Bisail B, et al. Comparison of ^{18}F -FDG and ^{67}Ga -citrate in sarcoidosis imaging. *Nuklearmedizin* 2008;47:18-23.
- Basu S, Zhuang H, Torigian DA, et al. Functional imaging of inflammatory diseases using nuclear medicine techniques. *Semin Nucl Med* 2009;39:124-45.
- Fazzi P, Solfanelli S, Begliomini E et al. ^{67}Ga scan, symptoms and treatment in sarcoidosis. *Sarcoidosis* 1993;10:155-6.
- Lynch JP, Kazerooni EA, Cay SE. Pulmonary sarcoidosis. In: Sharma O, Editor. *Clinics in chest medicine*. Philadelphia: Saunders; 1997. p. 755-85.
- Varghese RS, Bhugra P, Nicoleu C, Gumpeni R. Hepatic sarcoidosis presenting with stage 0 lung involvement, symptoms of cholestasis, hypercalcemia and renal insufficiency. *Chest* 2008;134:66C.
- Prasad V, Baum RP. Biodistribution of the Ga-68 labeled somatostatin analogue DOTA-NOC in patients with neuroendocrine tumors: characterization of uptake in normal organs and tumor lesions. *Q J Nucl Med Mol Imaging* 2010;54:61-7.
- Keijsers RG, van den Heuvel DA, Grutters JC. Imaging the inflammatory activity of sarcoidosis. *Eur Respir J* 2013;41:743-51.
- Chitambar CR. Medical applications and toxicities of gallium compounds. *Int J Environ Res Public Health* 2010;7:2337-61.
- Deppen SA, Liu E, Blume JD, et al. Safety and efficacy of ^{68}Ga -DOTATATE PET/CT for diagnosis, staging, and treatment management of neuroendocrine tumors. *J Nucl Med* 2016;57:708-14.
- Lococo F, Perotti G, Cardillo G, et al. Multicenter comparison

- of 18F-FDG and 68Ga-DOTA-peptide PET/CT for pulmonary carcinoid. *Clin Nucl Med* 2015;40:183-9.
22. Crown A, Rocha FG, Raghu P et al. Impact of initial imaging with gallium-68 dotatate PET/CT on diagnosis and management of patients with neuroendocrine tumors. *J Surg Oncol* 2020;121:480-5.
 23. Pollard J, McNeely P, Menda Y. Nuclear imaging of neuroendocrine tumors. *Surg Oncol Clin N Am* 2020;29:209-21.
 24. Deppen SA, Blume J, Bobbey AJ, et al. 68Ga-DOTATATE compared with 111In-DTPA-octreotide and conventional imaging for pulmonary and gastroenteropancreatic neuroendocrine tumors: A systematic review and meta-analysis. *J Nucl Med* 2016;57:872-8.
 25. Light RW, Macgregor MI, Luchsinger PC, et al. Pleural effusions: The diagnostic separation of transudates and exudates. *Ann Intern Med* 1972;77:507-13.
 26. Roth BJ, O'Meara TF, Cragun WH. The serum-effusion albumin gradient in the evaluation of pleural effusions. *Chest* 1990;98:546-9.
 27. Costa M, Quiroga T, Cruz E. Measurement of pleural fluid cholesterol and lactate dehydrogenase. A simple and accurate set of indicators for separating exudates from transudates. *Chest* 1995;108:1260-3.
 28. Meisel S, Shamiss A, Thaler M, et al. Pleural fluid to serum bilirubin concentration ratio for the separation of transudates from exudates. *Chest* 1990;98:141-4.

Non-commercial use only